Electronic Supplementary Information (ESI)

A highly stable chain-based Eu^{III} metal-organic framework as the turn-on and blue-shift luminescent sensor for 2,6-dipicolinic acid

Li Wang,[a] Yu-Lian Zhu,[b] Teng-Fei Zheng,[a] Zi-Hao Zhu,[a]* Yan Peng,[a] Yong-Quan Wu,[b] Jing-Lin Chen,[a] Sui-Jun Liu[a]* and He-Rui Wen[a]

[a]School of Chemistry and Chemical Engineering, Jiangxi Provincial Key Laboratory of Functional Molecular Materials Chemistry, Jiangxi University of Science and Technology, Ganzhou 341000, Jiangxi Province, P.R. China

[b]School of Chemistry and Chemical Engineering, Gannan Normal University, Ganzhou 341000, Jiangxi Province, P.R. China

---

*Corresponding authors. E-mail: sjliu@jxust.edu.cn (S.-J. Liu), zhuzihao@jxust.edu.cn (Z.-H. Zhu).

Materials and instrumentations

All chemical reagents were obtained from commercial sources and used without further purification. Notably, H_2BTDB was purchased by Jilin Chinese Academy of Sciences - Yanshen Technology Co., Ltd. and the NMR spectrum is provided in Fig. S1. The powder X-ray diffraction (PXRD) patterns were recorded by Rigaku MiniFlex 600. The simulated PXRD pattern of single-crystal data was obtained using the Mercury (Hg) software, which is freely available on the Internet at http://www.iucr.org. Thermogravimetric analysis (TGA) was performed under a N_2 flow at a heating rate of 10 K min^{-1} from 25 to 1000 °C on a NETZSCH STA2500 thermal analyzer. IR spectra in the range of 4000–400 cm^{-1} were collected with KBr particles on a Bruker Alpha FT-IR spectrometer. The fluorescence lifetime decays were recorded on a HORIBA Flourolog fluorescence spectrophotometer. The UV-vis adsorption spectra were collected on a UV-2550 (SHIMADZU) spectrophotometer. Scanning electron microscopy (SEM) was carried out on MLA650F SEM (FIE, USA).

Crystallographic studies for JXUST-38

Single crystal X-ray diffraction data of **JXUST-38** were recorded on a Bruker D8 QUEST diffractometer under 296(2) K and Mo-Kα radiation (λ = 0.71073 Å) by ω scan mode. SAINT program was used for diffraction profile integration.[S1] The SHELXT program of SHELXTL software package was used to solve the structure directly, and the full matrix least square method was used to refine the structure.[S2] The non-hydrogen atoms were situated in successive difference Fourier syntheses and refined by anisotropic thermal parameters on F^2. Theoretically, the hydrogen atoms of ligands are formed on specific atoms, and isotropic refinement was carried out by a fixed thermal factor.
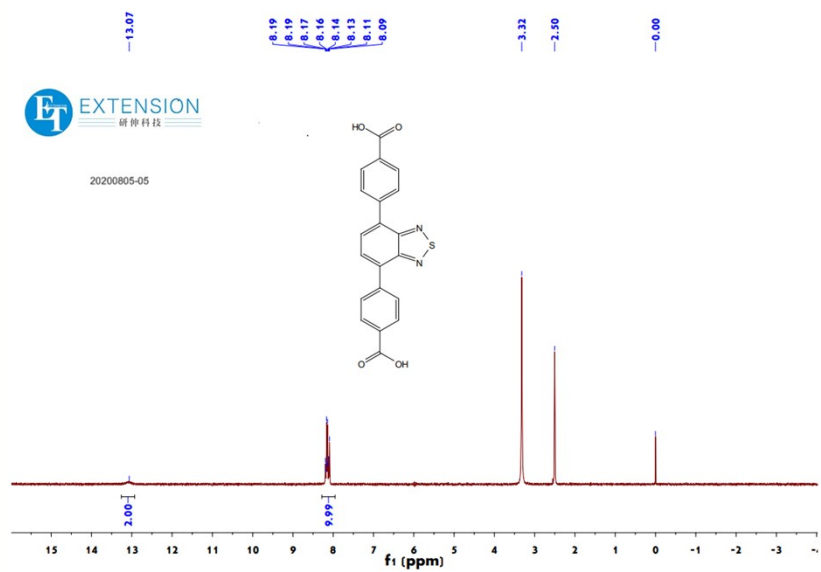
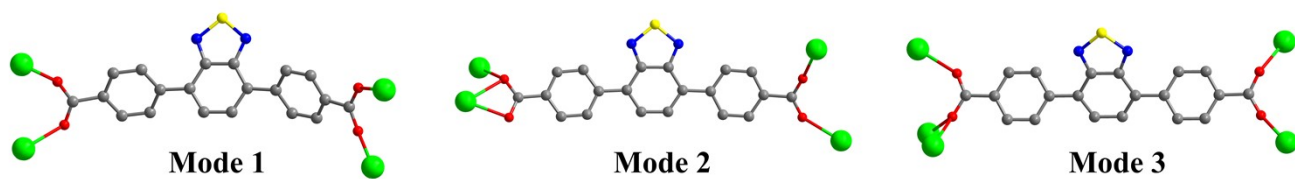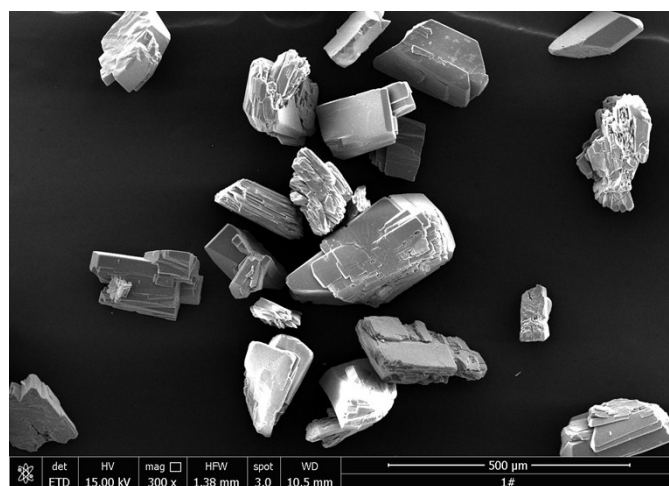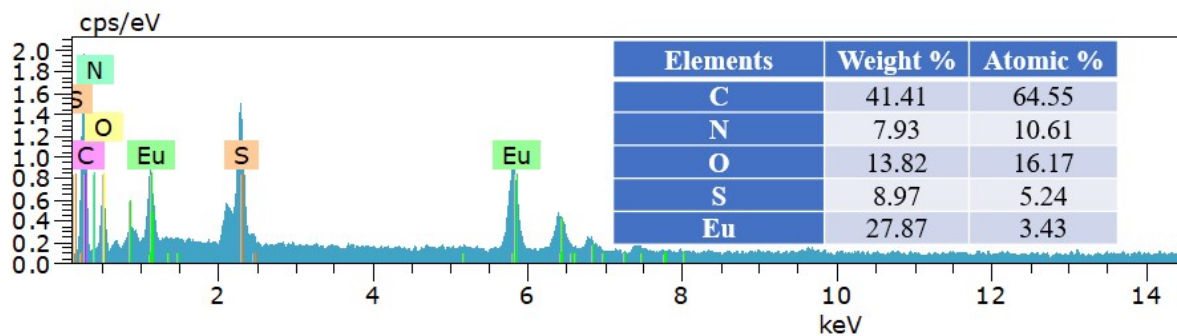**Fig. S1** NMR spectrum of the H₂BTDB ligand.

Fig. S2 The coordination modes of H₂BTDB ligand in **JXUST-38**.

(a)

3

(b)

Fig. S3 (a) Scanning electron microscopy of **JXUST-38**. (b) Elemental analysis from scanning electron microscope-energy dispersive X-ray analysis of **JXUST-38**.

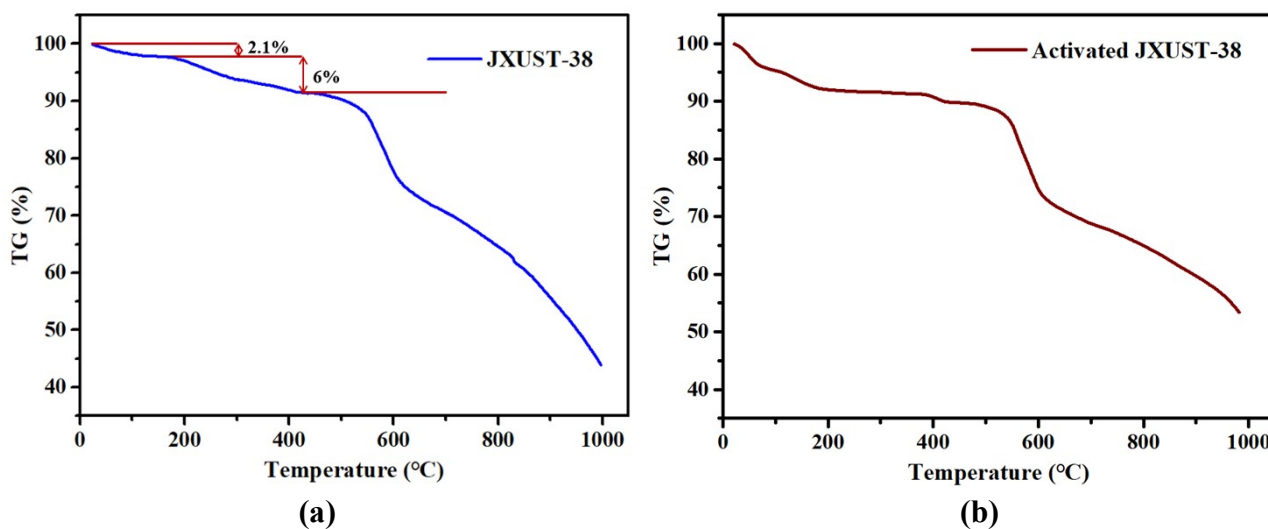| Elements	Weight %	Atomic %
C	41.41	64.55
N	7.93	10.61
O	13.82	16.17
S	8.97	5.24
Eu	27.87	3.43

(a)   **(b)**

Fig. S4 The TGA curves of (a) **JXUST-38** and (b) the activated **JXUST-38**.
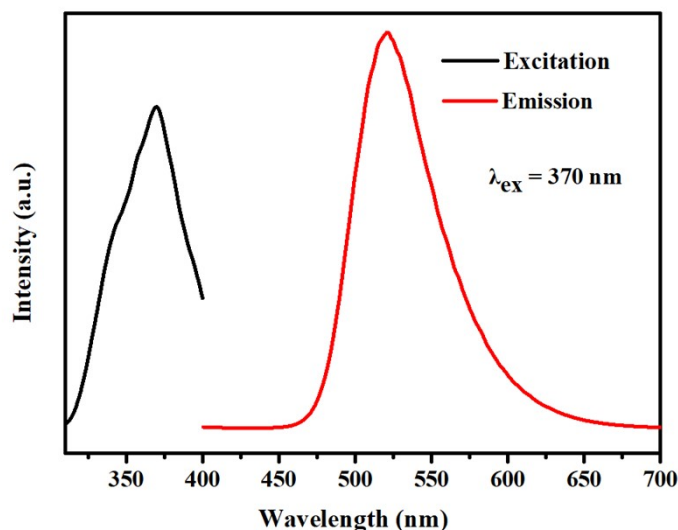

Fig. S5 The solid-state excitation and emission spectra of **JXUST-38**.
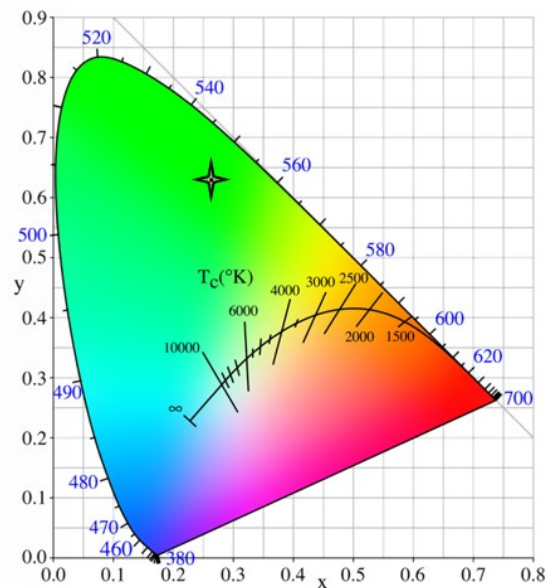
Fig. S6 CIE chromaticity diagram displaying the color coordinate of **JXUST-38**.
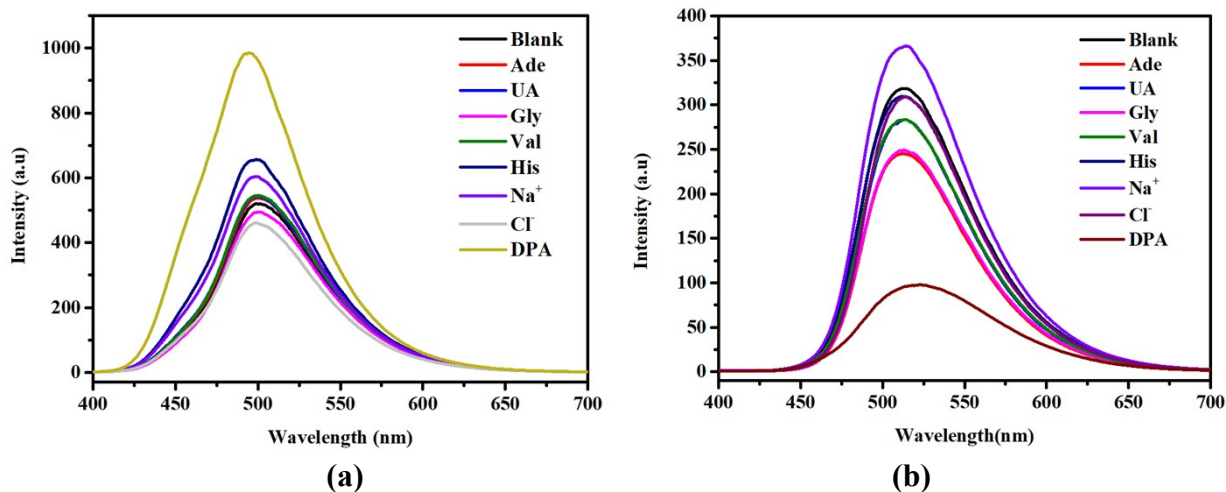

(a)

(b)

Fig. S7 Luminescence intensity with specific recognition of DPA in (a) EtOH and (b) aqueous solutions.
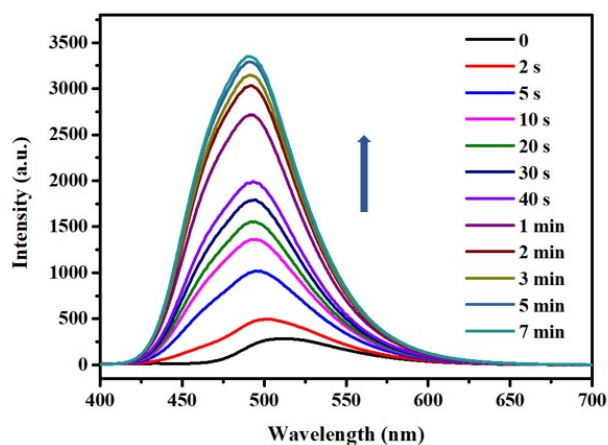
Fig. S8 Time-dependent emission spectra of **JXUST-38** after adding DPA at room temperature.
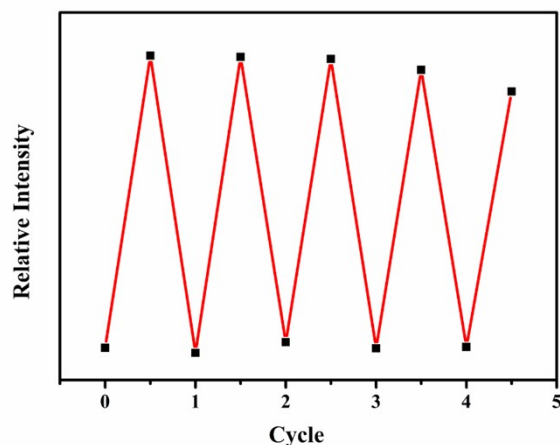
Fig. S9 Relative luminescent intensity of **JXUST-38** after five cycles of recycling experiments for DPA.

(a)   (b)
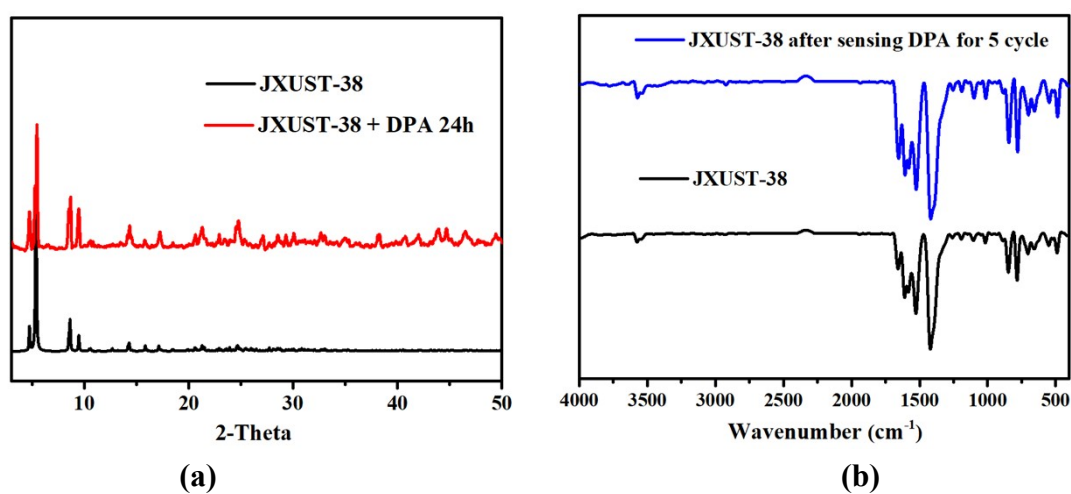
Fig. S10 (a) The PXRD patterns **JXUST-38** with the fresh sample and soaked in DMF solution containing DPA for 24 hours. (b) The IR spectra of **JXUST-38** and **JXUST-38** after sensing DPA for 5 cycles.

(a)   (b)
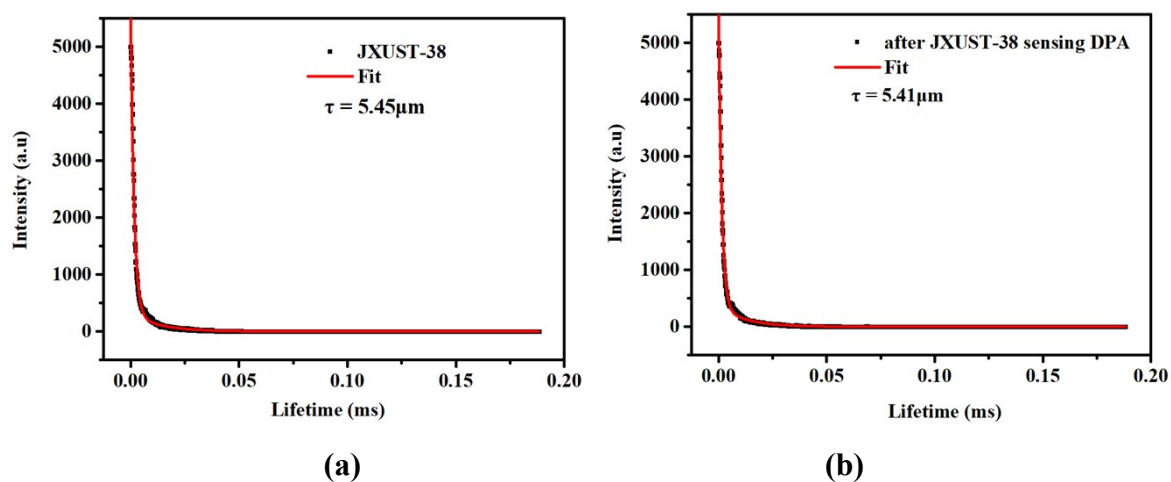
Fig. S11 The luminescence decay curves of (a) **JXUST-38** and (b) **JXUST-38**@DPA at room temperature.
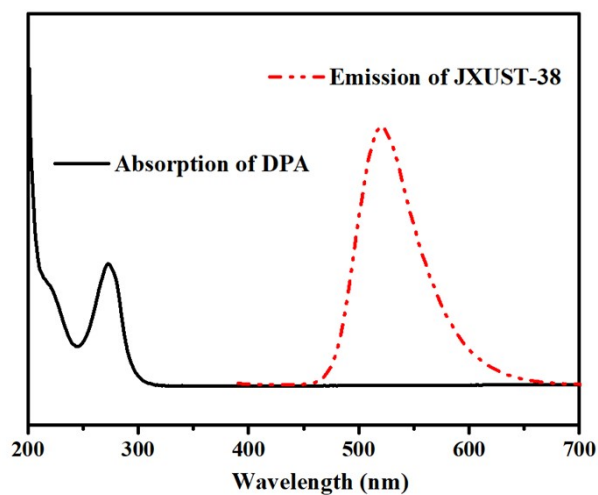
Fig. S12 The emission spectrum of **JXUST-38** and the UV-vis absorption spectrum of DPA.
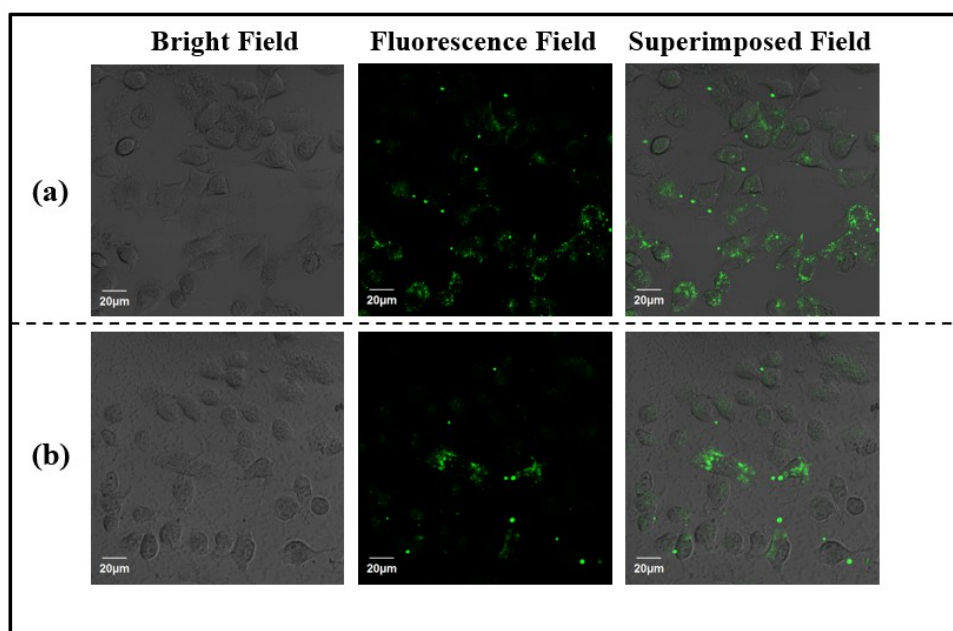
Fig. S13 Bright-field transmission image, fluorescence image and superimposed field image of (a) **JXUST-38** and (b) **JXUST-38**@DPA.
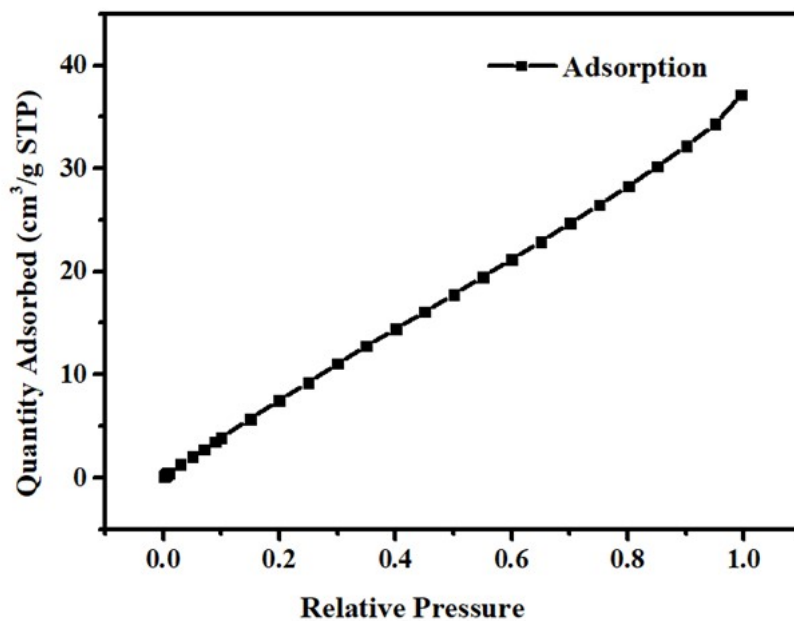
Fig. S14 The N$_2$ adsorption isotherms for **JXUST-38** at 77 K. **JXUST-38** does not exhibit a significant microporous structure based on the isotherms, which may be due to its lower porosity.

Table S1. Crystal data and structure refinements for **JXUST-38**.

Compound	JXUST-38
formula	$C_{60}H_{32}Eu_3N_6O_{16}S_3$
Mr	1644.97
T (K)	293(2)
crystal system	triclinic
space group	$P\bar{1}$
a (Å)	8.8463(3)
b (Å)	18.8634(7)
c (Å)	20.8662(7)
α (º)	113.6650(10)
β (º)	95.5710(10)
γ (º)	102.2300(10)
V (Å^3)	3051.60(19)
Z	2
$F(000)$	1598
D_{calc} (g cm^{-3})	1.79
μ (mm^{-1})	3.221
Reflections collected/unique	46674/13992
R_{int}	0.0259
$R_1{}^a/wR_2{}^b$ [$I>2\sigma(I)$]	0.0205
$R_1{}^a/wR_2{}^b$ (all data)	0.0263
GOF on F^2	1.047

$^aR_1 = \Sigma(||F_0| - |F_C||)/\Sigma|F_0|$; $^bwR_2 = [\Sigma w(|F_0|^2 - |F_C|^2)^2/(\Sigma w|F_0|^2)^2]^{1/2}$.

Table S2. Selected bond lengths (Å) and angles (°) for **JXUST-38**[a].

Eu1—O1	2.3360(18)	Eu2—O5[ii]	2.5215(16)
Eu1—O9	2.5018(18)	Eu2—O4	2.4349(17)
Eu1—O7	2.3009(17)	Eu2—O8[v]	2.3717(18)
Eu1—O5	2.5797(17)	Eu3—O3	2.3346(18)
Eu1—O14	2.3724(16)	Eu3—O9[vi]	2.6063(18)
Eu1—O13	2.4064(16)	Eu3—O6[v]	2.3420(16)
Eu1—O15	2.3694(14)	Eu3—O11[vii]	2.3414(18)
Eu1—O15[i]	2.3433(14)	Eu3—O10[vi]	2.4631(18)
Eu2—O2[ii]	2.4438(18)	Eu3—O15[v]	2.3694(14)
O1—Eu1—O5	74.12(6)	O2[ii]—Eu2—O5[ii]	71.44(6)
O1—Eu1—O14	98.79(7)	O4—Eu2—O2[ii]	107.96(6)
O1—Eu1—O13	83.80(6)	O4—Eu2—O5[ii]	79.04(6)
O1—Eu1—O15	148.22(6)	O8[vi]—Eu2—O2[ii]	73.21(7)
O1—Eu1—O15[i]	140.62(6)	O8[vi]—Eu2—O5[ii]	124.56(6)
O9—Eu1—O5	142.81(5)	O8[vi]—Eu2—O4	72.99(6)
O7—Eu1—O1	93.38(7)	O3—Eu3—O9[iv]	135.46(6)
O7—Eu1—O9	74.67(6)	O3—Eu3—O6[vi]	86.83(6)
O7—Eu1—O5	86.71(6)	O3—Eu3—O11[vii]	141.70(7)
O7—Eu1—O14	147.86(6)	O3—Eu3—O10[iv]	94.48(7)
O7—Eu1—O13	141.99(6)	O3—Eu3—O15[vi]	131.43(6)
O7—Eu1—O15	74.48(6)	O3—Eu3—O1W	72.31(8)
O7—Eu1—O15[i]	85.16(6)	O6[vi]—Eu3—O9[iv]	134.94(6)
O14—Eu1—O9	137.23(6)	O6[vi]—Eu3—O10[iv]	162.38(7)
O14—Eu1—O5	68.49(5)	O6[vi]—Eu3—O15[vi]	75.83(5)
O14—Eu1—O13	69.31(5)	O6[vi]—Eu3—O1W	84.89(8)
O13—Eu1—O9	67.95(6)	O11[vii]—Eu3—O9[iv]	74.29(6)
O13—Eu1—O5	128.00(5)	O11[vii]—Eu3—O6[vi]	78.05(6)
O151—Eu1—O9	66.49(5)	O11[vii]—Eu3—O10[iv]	90.34(7)
O15—Eu1—O9	126.90(6)	O11[vii]—Eu3—O15[vi]	78.68(6)
O15[i]—Eu1—O5	144.68(5)	O11[vii]—Eu3—O1W	71.45(8)
O15—Eu1—O5	75.91(5)	O10[iv]—Eu3—O9[iv]	51.24(6)
O15—Eu1—O14	79.69(5)	O15[vi]—Eu3—O9[iv]	64.41(5)
O15[i]—Eu1—O14	103.10(5)	O15[vi]—Eu3—O10[iv]	115.19(6)
O15[i]—Eu1—O13	74.09(5)	O15[vi]—Eu3—O1W	147.21(7)
O15—Eu1—O13	123.79(5)	O1W—Eu3—O9[iv]	117.90(7)
O15[i]—Eu1—O15	68.79(6)	O1W—Eu3—O10[iv]	78.82(8)
O1—Eu1—O9	75.16(6)		

[a]Symmetry codes: (i) 2-*x*, 1-*y*, 1-*z*; (ii) -*x*, -*y*, -*z*; (iii) 1+*x*, 1+*y*, 1+*z*; (iv) -1-*x*, -1-*y*, -1-*z*; (v) 1-*x*, -*y*, -*z*; (vi) -1+*x*, -1+*y*, -1+*z*. (vii) 1-*x*, -*y*, -1-*z*.

<p style="text-align:center">Table S3. SHAPE analysis of the Eu^{III} ions in JXUST-38.</p>

ions	label	Shape	symmetry	distortion(τ)
		JXUST-38		
	OP-8	Octagon	D_{8h}	30.380
	HPY-8	Heptagonal pyramid	C_{7v}	23.405
	HBPY-8	Hexagonal bipyramid	D_{6h}	15.601
	CU-8	Cube	O_h	10.762
	SAPR-8	Square antiprism	D_{4d}	3.679
	TDD-8	**Triangular dodecahedron**	**D_{2d}**	**1.110**
Eu1	JGBF-8	Johnson gyrobifastigium J26	D_{2d}	12.292
	JETBPY-8	Johnson elongated triangular bipyramid J14	D_{3h}	26.864
	JBTPR-8	Biaugmented trigonal prism J50	C_{2v}	2.533
	BTPR-8	Biaugmented trigonal prism	C_{2v}	2.548
	JSD-8	Snub diphenoid J84	D_{2d}	2.775
	TT-8	Triakis tetrahedron	T_d	11.216
	ETBPY-8	Elongated trigonal bipyramid	D_{3h}	24.465
	OP-8	Octagon	D_{8h}	32.300
	HPY-8	Heptagonal pyramid	C_{7v}	23.455
	HBPY-8	Hexagonal bipyramid	D_{6h}	12.413
	CU-8	Cube	O_h	5.993
	SAPR-8	**Square antiprism**	D_{4d}	**1.544**
	TDD-8	Triangular dodecahedron	**D_{2d}**	1.689
Eu2	JGBF-8	Johnson gyrobifastigium J26	D_{2d}	14.525
	JETBPY-8	Johnson elongated triangular bipyramid J14	D_{3h}	27.569
	JBTPR-8	Biaugmented trigonal prism J50	C_{2v}	3.402
	BTPR-8	Biaugmented trigonal prism	C_{2v}	2.972
	JSD-8	Snub diphenoid J84	D_{2d}	5.511
	TT-8	Triakis tetrahedron	T_d	6.870
	ETBPY-8	Elongated trigonal bipyramid	D_{3h}	24.253
Eu3	OP-8	Octagon	D_{8h}	29.650

HPY-8	Heptagonal pyramid	C_{7v}	22.341
HBPY-8	Hexagonal bipyramid	D_{6h}	14.032
CU-8	Cube	O_h	9.008
SAPR-8	Square antiprism	D_{4d}	2.376
TDD-8	Triangular dodecahedron	$\boldsymbol{D_{2d}}$	2.880
JGBF-8	Johnson gyrobifastigium J26	D_{2d}	12.027
JETBPY-8	Johnson elongated triangular bipyramid J14	D_{3h}	26.569
JBTPR-8	Biaugmented trigonal prism J50	C_{2v}	2.121
BTPR-8	**Biaugmented trigonal prism**	C_{2v}	**1.618**
JSD-8	Snub diphenoid J84	D_{2d}	4.692
TT-8	Triakis tetrahedron	T_d	9.675
ETBPY-8	Elongated trigonal bipyramid	D_{3h}	21.751

Table S4. Performance comparison of sensors for DPA detection.

Sensors	Linear ranges	LODs	Ref.
JXUST-38	0-78 μM	0.05 μM	**This work**
NH_2-MOF-76(Eu)	0-100 mM	3.8 μM	S3
$[Eu_{0.1}Tb_{0.9}(NDC^{2-})(H_2O)Cl]$	0-600 μM	0.248 μM	
$[Eu_{0.1}Tb_{0.9}(BDC^{2-})(H_2O)Cl]$	0-400 μM	0.874 μM	S4
$[Eu_{0.1}Tb_{0.9}(BDC^{2-})(H_2O)Cl]$	0-300 μM	2.277 μM	
[Tb(NDBC)(COO)]	0-1000 μM	5.21 μM	S5
$Tb_{0.875}Eu_{0.125}$-Hddb	0-400 μM	0.8494 μM	S6
Eu/Tb(BTC)	0-400 μM	1087 nM	S7
$[Tb_{0.43}Eu_{1.57}(1,4\text{-phda})_3(H_2O)](H_2O)_2$	0-400 μM	0.17 μM	S8
$\{[Ca_3(ddpa)\cdot 7H_2O]\}_n$	0-0.991 mM	1.01×10^{-6} M^{-1}	
$\{[Cd_3(ddpa)\cdot 6H_2O]\cdot 4H_2O\}_n$	0-0.991 mM	1.17×10^{-6} M^{-1}	S9
$\{[Zn_3(ddpa)\cdot 2H_2O]\}_n$	0-0.991 mM	2.07×10^{-6} M^{-1}	

References

S1   *SAINT*, *Version 6.02a*, Bruker AXS Inc, Madison, WI, 2002.

S2   G. M. Sheldrick, *Acta Crystallogr. Sect. A: Found. Adv.,* 2015, **A71**, 3-8.

S3   D. Wu, Z. Zhang, X. W. Chen, L. K. Meng, C. G Li, G. H. Li, X. B. Chen, Z. Shi and S. H. Feng, *Chem. Commun.*, 2019, **55**, 14918-14921.

S4   M. L. Shen, B. Liu, L. Xu and H. Jiao, *J. Mater. Chem. C*, 2020, **8**, 4392-4400.

S5   M. M. Qiu, K. F. Chen, Q. R. Liu, W. N. Miao, B. Liu and L. Xu, *CrystEngComm*, 2022, **24**, 132-142.

S6   X. B. Chen, C. X. Qi, Y. B. Xu, H. Li, L. Xu and B. Liu, *J. Mater. Chem. C*, 2020, **8**, 17325-17335.

S7   M. N. Wu, Y. X. Zhuang, J. B. Liu, W. W. Chen, X. Y. Li and R. J. Xie, *Opt. Mater.*, 2020, **106**, 110006.

S8   J. Othong, J. Boonmak, F. Kielar, S. Hadsadee, S. Jungsuttiwong and S. Youngme, *Sens. Actuators*, *B*, 2020, **316**, 128156.

S9   Z. Z. Cong, M. C. Zhu, Y, Zhang, W. Yao, Marina Kosinova, Vladimir P. Fedin, S. Y. Wu and E. J. Gao, *Dalton Trans.*, 2022, **51**, 250–256.